Appl Phys B (2009) 95: 237–244
DOI 10.1007/s00340-009-3457-4

Applied Physics B
Lasers and Optics

Nonclassical correlations from dissociation-time entanglement

C. Gneiting · K. Hornberger

Received: 30 September 2008 / Published online: 14 March 2009

Abstract We discuss a strongly entangled two-particle state of motion that emerges naturally from the double-pulse dissociation of a diatomic molecule. This state, which may be called dissociation-time entangled, permits the unambiguous demonstration of nonclassical correlations by violating a Bell inequality based on switched single-particle interferometry and only position measurements. We apply time-dependent scattering theory to determine the detrimental effect of dispersion. The proposed setup brings into reach the possibility of establishing nonclassical correlations with respect to system properties that are truly macroscopically distinct.

PACS 03.67.Bg · 37.25.+k · 03.65.Ud

1 Introduction

Quantum mechanics (QM) has been forcing physicists to think about its relation to our classical perception of the world ever since its formulation. Probably its most unsettling feature is the rejection of the notion of the trajectory of a proper, material particle. The at every instant well-defined, definite position of a point particle in space (or rather phase space), as we deduce it from our everyday experience of the macroscopic world, is probably the most basic assumption in classical physics; it might rightly be called its core. Quantum mechanics, on the other hand, permits superpositions of arbitrarily remote positions of a particle. The second cornerstone of classical physics, locality, is equally abandoned in QM by entanglement, which entails correlations between spatially separated parties that cannot be reduced to shared randomness [1–4]. So what could be a more striking demonstration of the failure of classical concepts than the experimental generation of a state that combines both, particles simultaneously being at macroscopically distinct positions and being entangled in these positions? In this article, we would like to promote such a state, whose experimental demonstration seems to be in reach of present day technology.

The approach is to trigger the dissociation of a diatomic molecule coherently at two different instants ("early" and "late") separated by a time period τ, as depicted in Fig. 1(a). The dissociation is coherent in the sense that no information is leaked to the environment about the time of dissociation. Each atom then has an early and a late wave packet component such that the resulting state of two counterpropagating particles is entangled in the dissociation times. For this reason, such a state might be called "dissociation-time entangled" (DTE). A macroscopic time period τ would result in a superposition of truly macroscopically distinct wave packets. Experimental setups based on ultracold Feshbach molecules indeed render such a scenario realistic [5].

Of course, generating a highly nonclassical state is only half of the job to be done. Just as important is the verification of its nonclassical nature. Here a subtlety comes into play: Whom do we want to convince? Do we face a person that believes in QM, or do we face a cocksure classical physicist, who understands how to measure a particle position but knows nothing about quantum physics? Several proposals for demonstrating nonclassicality in the motion of material particles are content with the confirmation of the entangled nature of the underlying quantum states, while suffering from the caveat that they have to presume the validity of QM

C. Gneiting · K. Hornberger (✉)
Arnold Sommerfeld Center for Theoretical Physics,
Ludwig-Maximilians-Universität München, Theresienstraße 37,
80333 Munich, Germany
e-mail: Hornberger@lmu.de

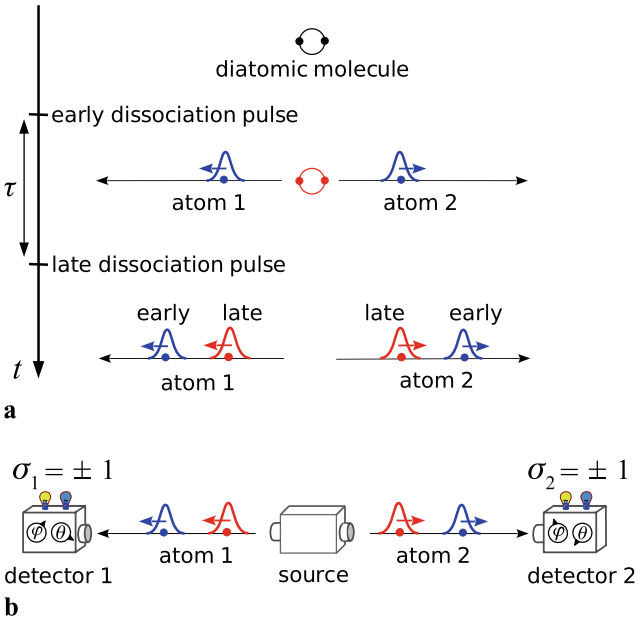

Fig. 1 (**a**) Generation of a dissociation-time entangled pair of atoms. A diatomic molecule is exposed to two subsequent dissociation pulses separated by a time period τ. The early pulse is chosen such that the atoms remain bound with a given probability. The second pulse dissociates the remaining molecular state component. Each atom then has an early and a late wave packet component such that the resulting state of two counterpropagating particles is entangled in the dissociation times. (**b**) If the wave packet components of the dissociation-time entangled atoms are spatially sufficiently separated, they constitute effectively dichotomic properties which are amenable to a Bell test in terms of switched single-particle interferometry and position measurements, see Fig. 2

in order to be convincing. From an operational point of view, they do not imply nonclassicality by establishing nonlocal correlations. They therefore fail to convince the cocksure classical physicist—or an unprejudiced layman. This holds in particular for proposals that are close in spirit to the original Einstein–Podolsky–Rosen (EPR) argument [1, 6, 7], since the positive Wigner function of the EPR state admits a classical interpretation. One possibility to overcome this would be to consider observables which have no classical analogue, such as the displaced parity or pseudospin operators, with nonpositive phase space representations [8, 9]. However, their experimental implementation seems to be exceedingly difficult in the case of free material particles, where only position measurements are easily realized.

The DTE state differs fundamentally from the Gaussian states describing EPR-type correlations. As opposed to Gaussian states, it displays a strongly structured, partly negative Wigner function, and it is amenable to an unambiguous demonstration of nonclassicality in terms of simple position measurements. This is achieved by implementing a Bell experiment, as will be elaborated below, see Fig. 1(b). Within a range of tolerance as imposed by dispersion, the resulting nonlocal correlations would manifest both the coherence between the macroscopically distinct early and late wave packet components and their entanglement. The proposed setup would therefore permit the demonstration of nonclassicality in the motion of material particles on macroscopic scales, making quantum mechanical counterintuitiveness concrete for anyone, even the layman.

The article is structured as follows: In Sect. 2 we recall the concept of time-bin entanglement, which was originally applied to photons [10–12]. We carry it over to material particles and discuss the implications for a Bell test based on interferometric state transformation and subsequent detection. In particular, we show why the dispersion-induced spreading of the wave packets, which is absent in the photonic case, does not diminish the ensuing nonlocal correlations. In Sect. 3 we investigate the analogue Bell test based on dissociation-time entanglement, which corresponds to the more natural state generation scenario. The dispersion-induced distortion between the early and the late wave packets is shown to affect the nonlocal correlations. We give benchmark criteria for the capability of establishing nonclassicality. In Sect. 4 we finally summarize the advantages of a demonstration of nonclassicality based on a DTE Bell test, which includes in particular the possibility to go to macroscopic scales.

2 Time-bin entanglement

The idea to encode qubits in spatially distinct wave packets was introduced in [10], building upon the concept of energy-time entanglement [13]. A pulsed laser in combination with an asymmetric interferometer placed in front of a parametric down-conversion crystal permits to generate twin-photons which are entangled in their creation time. The resulting state, which may be called time-bin entangled (TBE), takes the form

$$|\Psi_{\mathrm{tbe}}\rangle = \frac{1}{\sqrt{2}}\big(|\mathrm{E}\rangle_1|\mathrm{E}\rangle_2 + \mathrm{e}^{\mathrm{i}\phi_\tau}|\mathrm{L}\rangle_1|\mathrm{L}\rangle_2\big), \tag{1}$$

where $|\mathrm{E}\rangle_i$ and $|\mathrm{L}\rangle_i$ denote spatially distinct traveling photonic modes corresponding to the early and the late creation time. The TBE state (1) can be visualized analogously to the DTE state depicted in Fig. 1(b). Since the relevant entanglement resides in the relation between these modes, we can interpret the creation times as a dichotomic property constituting an effectively two-dimensional state space (per photon). By identifying, say, "early" with "spin up" and "late" with "spin down," the state $|\Psi_{\mathrm{tbe}}\rangle$ evidently corresponds to the Bell state

$$|\Psi_{\mathrm{spin}}\rangle = \frac{1}{\sqrt{2}}\big(|\uparrow\rangle_1|\uparrow\rangle_2 + \mathrm{e}^{\mathrm{i}\phi}|\downarrow\rangle_1|\downarrow\rangle_2\big). \tag{2}$$

Provided that the early and the late wave packet components are spatially sufficiently distinct, a switched, asymmetric

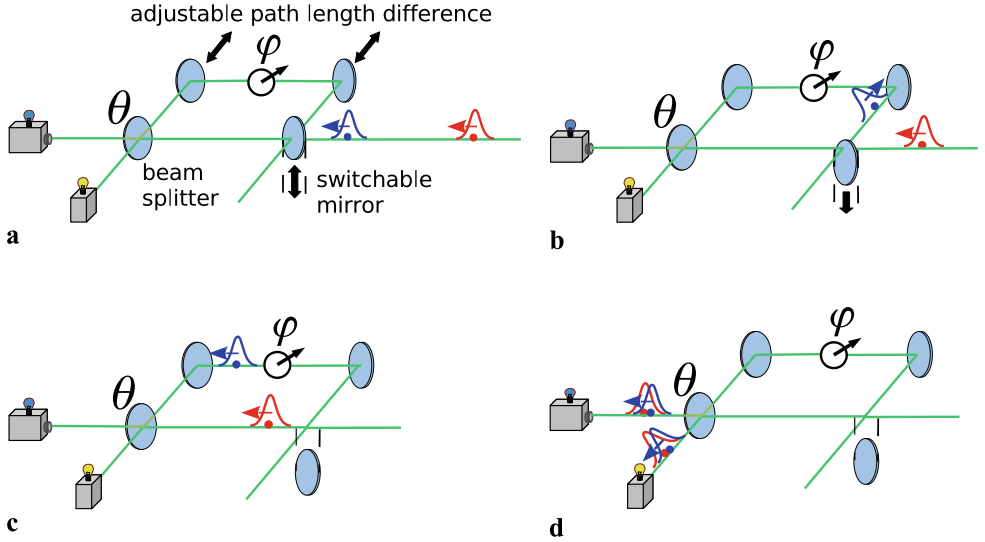

Fig. 2 State analysis with an asymmetric Mach–Zehnder interferometer. (**a**) When the early wave packet component arrives, the switchable mirror is in place and deflects it into the long arm. (**b**) The switchable mirror is removed before the arrival of the late wave packet. (**c**) The early wave packet acquires an optional phase shift φ in the long arm, whereas the late wave packet propagates through the short arm. (**d**) The path difference is chosen such that it cancels the distance between the early and the late wave packet component. Detecting the atom in one of the output ports, at a given phase φ and splitting ratio θ, amounts to a measurement analogous to a spin-1/2 detection in an arbitrary direction

Mach–Zehnder interferometer makes it possible to perform the analogue of a general spin measurement, see Fig. 2 and the discussion below [10]. Such a TBE state has indeed been used successfully with photons, e.g., for establishing nonlocal correlations over fiber distances of more than 50 km [10–12] in a similar setup as in Fig. 2, though without switching.

The matter wave analogue of the TBE state (1) follows from identifying $|\mathrm{E}\rangle_i$ and $|\mathrm{L}\rangle_i$ with the early and the late wave packet components of two freely moving atoms. It should be emphasized, though, that when it comes to material particles, the TBE state (1) is not the natural outcome in a two-time dissociation process. One conceivable scenario relies on the controlled dissociation of a weakly bound Feshbach molecule with the help of a Feshbach resonance [5]. An appropriately chosen magnetic field pulse causes the atomic components to dissociate and propagate in opposite directions [14, 15]. A sequence of two magnetic field pulses then generates the desired superposition of two dissociation times. A generic dissociation-time entangled (DTE) state thus takes the form

$$|\Psi_{\mathrm{dte}}\rangle = \frac{1}{\sqrt{2}}\left(\hat{\mathrm{U}}_{\tau}^{(0)}|\Psi_0\rangle + \mathrm{e}^{\mathrm{i}\phi_\tau}|\Psi_0\rangle\right) \tag{3}$$

with $|\Psi_0\rangle = \frac{1}{\sqrt{2}}|\psi_0^{\mathrm{cm}}\rangle(|\psi_0^{\mathrm{rel}}\rangle + \hat{\mathrm{P}}|\psi_0^{\mathrm{rel}}\rangle)$. Here, $\hat{\mathrm{P}}$ is the parity operator, and we assume that the early and the late dissociation occur with equal probability. In the following, we take the state $|\Psi_{\mathrm{dte}}\rangle$, and accordingly $|\Psi_{\mathrm{tbe}}\rangle$, to describe a one-dimensional, longitudinal motion, implying that the transverse components of the motion are confined to the ground state of an atom guide. The state $|\psi_0^{\mathrm{rel}}\rangle$ denotes the wave packet of the relative motion after a single dissociation pulse propagating into positive direction, while $|\psi_0^{\mathrm{cm}}\rangle$ describes the wave packet of the center of mass motion resting at the former position of the molecule. The DTE state (3) differs from the above TBE state (1) as it is not composed of two single-particle product states. Rather, it superposes the relative coordinate of the two atoms. It also incorporates the unavoidable dispersion-induced distortion between the early and the late state components, described by the free time-evolution operator $\hat{\mathrm{U}}_{\tau}^{(0)}$.

Both the TBE state (1) and the DTE state (3) are amenable to a Bell test based on interferometric state transformation and subsequent position measurement. Before tackling the motional Bell experiment with the experimentally appropriate DTE state (3), it is instructive to first describe the interferometric setup and the effect of dispersion with the more transparent TBE state (1). The setup is based on switched, asymmetric Mach–Zehnder interferometers, as shown in Fig. 2. Their action can be described as follows: The early wave packet components are deflected by the switches into the long arms of the interferometers, where they acquire optional phase shifts φ_i before the beam splitters distribute them onto their output ports according to their splitting ratios, as parameterized by the angles θ_i. The switches are timed such that they let pass the late wave packet components, which then propagate straight to the beam splitters and are also distributed according to the splitting ratios. When the path length difference between the two

interferometer arms is chosen such that it exactly cancels the distance between the early and the late wave packets and given ideal phase shifters and beam splitters, the early and late state components $|\mathrm{E}\rangle_i$ and $|\mathrm{L}\rangle_i$ transform according to

$$\begin{aligned} |\mathrm{E}\rangle_i &\to \mathrm{e}^{\mathrm{i}\varphi_i}\cos\theta_i|+\rangle_i + \mathrm{e}^{\mathrm{i}\varphi_i}\sin\theta_i|-\rangle_i \\ |\mathrm{L}\rangle_i &\to \sin\theta_i|+\rangle_i - \cos\theta_i|-\rangle_i, \end{aligned} \tag{4}$$

where $|+\rangle_i$ and $|-\rangle_i$ denote wave packet components in the two output ports of the ith interferometer at a stage of the time evolution when the particles already passed the interferometers. This mapping assumes that the components $|\mathrm{E}\rangle_i$ and $|\mathrm{L}\rangle_i$ of the initial state are identical wave packets up to their spatial displacement: $|\mathrm{L}\rangle_i = \mathrm{e}^{\mathrm{i}\hat{\mathrm{p}}_i s_i/\hbar}|\mathrm{E}\rangle_i$, with s_i denoting their separation. Moreover, the states $|\mathrm{E}\rangle_i$ and $|\mathrm{L}\rangle_i$ must be sufficiently spatially distinct, such that they can be distinguished by the switches, even when taking dispersion-induced wave packet spreading into account. Note that it is not important to be specific about the particular instant, at which we consider the wave packet components $|+\rangle_i$ and $|-\rangle_i$, since we will only be interested in the overall detection probabilities per port, which unitary time evolution guarantees to remain unaffected by any subsequent time evolution. In this sense, the present treatment already incorporates dispersion, since we do not have to assume that the wave packets $|+\rangle_i$ and $|-\rangle_i$ are equal in shape to the wave packets $|\mathrm{E}\rangle_i$ and $|\mathrm{L}\rangle_i$.

After passing the interferometers, the time-bin entangled state can be written in accordance with (4) as

$$\big|\Psi'_{\mathrm{tbe}}\big\rangle = \frac{1}{2^{3/2}}\sum_{\sigma_1,\sigma_2=\pm}\big[\mathrm{e}^{\mathrm{i}(\varphi_1+\varphi_2)} + \sigma_1\sigma_2\mathrm{e}^{\mathrm{i}\phi_\tau}\big]|\sigma_1\rangle_1|\sigma_2\rangle_2. \tag{5}$$

For clarity, we have taken 50:50 beam splitters ($\theta_1 = \theta_2 = \pi/4$). As we will see, this restriction does not come with any loss of significance, since it still allows for a maximal violation of a Bell inequality. The joint probability for detecting the particles in a particular output port combination thus reads ($\sigma_{1,2} = \pm 1$)

$$\begin{aligned} &\mathrm{P}_{\mathrm{tbe}}(\sigma_1,\sigma_2|\varphi_1,\varphi_2) \\ &\quad = \big|\langle\sigma_1|_1\langle\sigma_2|_2\big|\Psi'_{\mathrm{tbe}}\big\rangle\big|^2 \\ &\quad = \frac{1}{4}\big[1+\sigma_1\sigma_2\cos(\varphi_1+\varphi_2-\phi_\tau)\big]. \end{aligned} \tag{6}$$

From an experimental point of view, the natural quantity to be measured is the arrival time of the particles at the detectors. The two-time probability density $\mathrm{pr}(\sigma_1,\sigma_2;t_1,t_2)$ for detecting the particles at times t_1, t_2 in a particular output port combination constitutes in general a complicated fringe pattern as a function of the φ_i, θ_i, and t_i. It depends not only on the shape of the wave packets and their dispersion-induced modifications due to the overall propagation time, but also on the particular implementation of the measurement [16–19]. The integrated probability $\mathrm{P}_{\sigma_1,\sigma_2} = \int \mathrm{d}t_1\,\mathrm{d}t_2\,\mathrm{pr}(\sigma_1,\sigma_2;t_1,t_2)$, however, only measures the overall likelihood for finding the particles in a particular output port combination. It is thus unaffected by the particular shape of the wave packets and any dispersion-induced modification thereof, since unitary time evolution implies the conservation of probability in the output ports. Strictly speaking, this is valid only if measurement-induced reflections of the wave packets at the detectors can be excluded [16–19]. But since our setup does not require prominent temporal or spatial resolution of the measurement, we can safely neglect this effect. For this reason, we may identify the integrated probability $\mathrm{P}_{\sigma_1,\sigma_2}$ with (6). From the joint probability (6) we easily obtain the corresponding correlation function:

$$\begin{aligned} C_{\mathrm{tbe}}(\varphi_1,\varphi_2) &= \sum_{\sigma_1,\sigma_2=\pm}\sigma_1\sigma_2\mathrm{P}_{\mathrm{tbe}}(\sigma_1,\sigma_2|\varphi_1,\varphi_2) \\ &= \cos(\varphi_1+\varphi_2-\phi), \end{aligned} \tag{7}$$

which violates the CHSH-inequality [20] $|C(\varphi_1,\varphi_2) + C(\varphi_1,\varphi'_2) + C(\varphi'_1,\varphi_2) - C(\varphi'_1,\varphi'_2)| \leqslant 2$ maximally, e.g., for the choices $\varphi_1 = \phi/2$, $\varphi_2 = \phi/2 - \pi/4$, $\varphi'_1 = \phi/2 + \pi/2$, and $\varphi'_2 = \phi/2 + \pi/4$.

Like for the (switched) photonic TBE Bell setup, the TBE correlation function for the material particles (7) is identical to the correlation function obtained in the spin-based Bell experiment with the state (2). We thus find that the nonlocal correlations due to the TBE state (1) are not affected by dispersion. This follows from the assumption that the early and the late wave packets are identical up to a spatial displacement. We will see below that this is not valid for the more realistic DTE state (3), where the dispersion-induced distortion between the early and the late wave packets is taken into account. We note that the photonic experiments performed to date have been done without switch, using instead a post-selection procedure [10]. This has been shown to allow for a local hidden variable model [21, 22], a drawback that is avoided if the switching can be easily implemented, as is the case with slow material particles.

In order to make the correspondence with the spin-based Bell experiment most transparent, we conclude this section by recalling that the above state transformation (4) acting on a general (single-particle) "time-bin" superposition state $|\psi\rangle = a|\mathrm{E}\rangle + b|\mathrm{L}\rangle$, $|a|^2 + |b|^2 = 1$, followed by the detection in one of the output ports can formally be understood as the analogue of a "spin" measurement with respect to the measurement axis $\vec{n} = (\sin(2\theta)\cos\varphi, \sin(2\theta)\sin\varphi, \cos(2\theta))$. To this end, we define the analogues of Pauli matrices

$$\begin{aligned} \hat{\sigma}_x &= |\mathrm{E}\rangle\langle\mathrm{L}| + |\mathrm{L}\rangle\langle\mathrm{E}|, \\ \hat{\sigma}_y &= -i|\mathrm{E}\rangle\langle\mathrm{L}| + i|\mathrm{L}\rangle\langle\mathrm{E}|, \\ \hat{\sigma}_z &= |\mathrm{E}\rangle\langle\mathrm{E}| - |\mathrm{L}\rangle\langle\mathrm{L}|, \end{aligned}$$

and $\hat{\vec{\sigma}} = (\hat{\sigma}_x, \hat{\sigma}_y, \hat{\sigma}_z)$. The interferometric transformation (4) and the subsequent detection of the transformed state $|\psi'\rangle$ in the output ports can then be equivalently understood as a measurement of the observable $\vec{n} \cdot \hat{\vec{\sigma}}$ with the untransformed state $|\psi\rangle$. This is most easily seen by noting that the transformation (4) acts like an expansion of the incoming time-bin state into the eigenstates $|\vec{n}, +\rangle, |\vec{n}, -\rangle$ of $\vec{n} \cdot \hat{\vec{\sigma}}$. With this, the joint detection probability may equally well be written as

$$\mathrm{P}_{\mathrm{tbe}}(\sigma_1, \sigma_2 | \vec{n}_1, \vec{n}_2) = \left| \langle \vec{n}_1, \sigma_1 |_1 \langle \vec{n}_2, \sigma_2 |_2 | \Psi_{\mathrm{tbe}} \rangle \right|^2,$$

and the correlation function is given by

$$C_{\mathrm{tbe}}(\vec{n}_1, \vec{n}_2) = \langle \Psi_{\mathrm{tbe}} | \left[\vec{n}_1 \cdot \hat{\vec{\sigma}}_1 \right] \otimes \left[\vec{n}_2 \cdot \hat{\vec{\sigma}}_2 \right] | \Psi_{\mathrm{tbe}} \rangle.$$

This correspondence implies that the above time-bin scenario can be used to apply other quantum information strategies to the motion of material particles, such as the teleportation of a qubit state. Encoding qubits in spatially distinct wave packets thus permits general single-qubit state processing to be based only on matter wave optics and subsequent position measurements. This gives us a simple and robust method at hand for performing the most relevant quantum tests in the *motion* of material particles.

3 Dissociation-time entanglement

Up to now, we mainly investigated the Bell test for the TBE state (1). However, from an experimental point of view, the DTE state (3) is much more relevant, since its structure is naturally produced by the dissociation of a diatomic molecule. The DTE wave function differs from the TBE state in two important points: (i) it does not separate into single-particle states at a particular dissociation time and (ii) the dispersive time evolution between the early and the late dissociation process implies different shapes for the early and late wave packet components. Furthermore, we now specify the phase shifters to be implemented by varying the arm lengths of the interferometers, which effects an additional mismatch between the early and the late state components. All these modifications require a more sophisticated theoretical description of the setup. It turns out that time-dependent scattering theory provides the appropriate framework.

Scattering theory applies when the system dynamics under consideration permits to relate asymptotic *in*-states to asymptotic *out*-states [23]. Then, given one is only interested in the relation between these asymptotic states, the exact time evolution connecting the *in* and the *out* states can be split up into an "instantaneous" transformation describing the accumulated effect of the interaction potential and a subsequent free time evolution. In our case,

$$\left| \Psi'_{\mathrm{dte}} \right\rangle := \hat{\mathrm{U}}_t | \Psi_{\mathrm{dte}} \rangle = \hat{\mathrm{U}}_t^{(0)} \hat{\mathrm{S}} | \Psi_{\mathrm{dte}} \rangle,$$

where $|\Psi'_{\mathrm{tbe}}\rangle$ denotes the TBE state at a given stage of evolution when the passage through the interferometers is completed, and the scattering operator $\hat{\mathrm{S}}$ describes the "raw" action of the interferometers. In our case, another subtlety comes into play, since we have to distinguish the effect of the interferometers depending on whether the switch is in place ("on"), enforcing deflection into the longer arm, as for the early state component, or absent ("off"), admitting undeflected passage, as for the late state component:

$$\left| \Psi'_{\mathrm{dte}} \right\rangle = \hat{\mathrm{U}}_t^{(0)} \left(\hat{\mathrm{S}}^{(\mathrm{on})} \hat{\mathrm{U}}_\tau^{(0)} \left| \Psi_0 \right\rangle + \mathrm{e}^{\mathrm{i}\phi_\tau} \hat{\mathrm{S}}^{(\mathrm{off})} \left| \Psi_0 \right\rangle \right).$$

Here we presuppose that dispersion-induced spreading does not spoil the spatial distinctness of the early and the late wave packets. In order to specify the structure of the scattering matrices $\hat{\mathrm{S}}^{(\mathrm{on})}$ and $\hat{\mathrm{S}}^{(\mathrm{off})}$, it is convenient to rewrite the DTE state (3) as

$$|\Psi_{\mathrm{dte}}\rangle = \frac{1}{\sqrt{2}} \left(\left| \Psi_{\mathrm{dte}}^{(+)} \right\rangle + \left| \Psi_{\mathrm{dte}}^{(-)} \right\rangle \right)$$

with

$$\left| \Psi_{\mathrm{dte}}^{(+)} \right\rangle = \frac{1}{\sqrt{2}} \left(\hat{\mathrm{U}}_\tau^{(0)} \left| \Psi_0^{(+)} \right\rangle + \mathrm{e}^{\mathrm{i}\phi_\tau} \left| \Psi_0^{(+)} \right\rangle \right),$$

where $|\Psi_0^{(+)}\rangle = |\psi_0^{\mathrm{cm}}\rangle |\psi_0^{\mathrm{rel}}\rangle$ and $|\Psi_{\mathrm{dte}}^{(-)}\rangle = \hat{\mathrm{P}} |\Psi_{\mathrm{dte}}^{(+)}\rangle$. Now $|\Psi_{\mathrm{dte}}^{(+)}\rangle$ describes a two-particle state with particle 1 (resp. particle 2) exclusively propagating into positive (negative) direction. This allows one to assign each particle to a definite interferometer, e.g., interferometer 1 to particle 1 (and interferometer 2 to particle 2). The same applies to $|\Psi_{\mathrm{dte}}^{(-)}\rangle$, only with the particles exchanged. Focusing on $|\Psi_{\mathrm{dte}}^{(+)}\rangle$, the projection of the scattered state $|\Psi_{\mathrm{dte}}^{(+)'}\rangle$ onto a particular output-port combination σ_1, σ_2 reads

$$\begin{aligned} &\left(\hat{\Pi}_{\sigma_1} \otimes \hat{\Pi}_{\sigma_2} \right) \left| \Psi_{\mathrm{dte}}^{(+)'} \right\rangle \\ &= \frac{\hat{\mathrm{U}}_t^{(0)}}{\sqrt{2}} \left\{ \hat{\mathrm{U}}_\tau^{(0)} \left[\hat{\mathrm{S}}_{\sigma_1}^{(\mathrm{on})} \otimes \hat{\mathrm{S}}_{\sigma_2}^{(\mathrm{on})} \right] \left| \Psi_0^{(+)} \right\rangle \right. \\ &\quad \left. + \mathrm{e}^{\mathrm{i}\phi_\tau} \left[\hat{\mathrm{S}}_{\sigma_1}^{(\mathrm{off})} \otimes \hat{\mathrm{S}}_{\sigma_2}^{(\mathrm{off})} \right] \left| \Psi_0^{(+)} \right\rangle \right\}. \end{aligned} \tag{8}$$

Here, $\hat{\Pi}_{\sigma_i}$ is the projection operator onto the region behind the output port labeled by $\sigma_i = (\pm)_i$ of the ith interferometer. The scattering matrix components $\hat{\mathrm{S}}_{\sigma_i}^{(\mathrm{on/off})} = \hat{\Pi}_{\sigma_i} \hat{\mathrm{S}}_i^{(\mathrm{on/off})}$ describe the mapping from an *in*-state to the *out*-state component of a particular beam splitter output port. For example, $\hat{\mathrm{S}}_{\sigma_1=+1}^{(\mathrm{on})} |\mathrm{in}\rangle$ yields the *out*-state component in the output port labeled by $\sigma_1 = +1$ with the switch in place ("on"). For the early wave packets, the switch is in place, causing deflection into the long arm. The offset from the optimum path length difference is reflected in a translation of

the early wave packets with respect to the late ones. The late wave packets, on the other hand, pass straight through the short arm before they are distributed into the output ports according to the splitting ratio of the beam splitter. For the scattering matrix components $\hat{\mathrm{S}}^{(\mathrm{on})}_{\sigma_i}$ and $\hat{\mathrm{S}}^{(\mathrm{off})}_{\sigma_i}$, one thus obtains

$$\begin{aligned}
\hat{\mathrm{S}}^{(\mathrm{on})}_{\sigma_i=+1} &= \mathrm{e}^{\mathrm{i}\hat{p}_i\ell_i/\hbar}\cos\theta_i,\\
\hat{\mathrm{S}}^{(\mathrm{on})}_{\sigma_i=-1} &= \mathrm{e}^{\mathrm{i}\hat{p}_i\ell_i/\hbar}\sin\theta_i,\\
\hat{\mathrm{S}}^{(\mathrm{off})}_{\sigma_i=+1} &= \sin\theta_i,\\
\hat{\mathrm{S}}^{(\mathrm{off})}_{\sigma_i=-1} &= -\cos\theta_i,
\end{aligned} \tag{9}$$

where the translation operators $\exp(\mathrm{i}\hat{p}_i\ell_i/\hbar)$ implement the additional displacements ℓ_i of the early state component (switch "on") with respect to the late ones. Like for the TBE state, the joint probability for detecting the particles in a particular output-port combination σ_1, σ_2 is obtained from $\mathrm{P}^{(+)}_{\mathrm{dte}}(\sigma_1,\sigma_2|\ell_1,\ell_2) = |(\hat{\Pi}_{\sigma_1}\otimes\hat{\Pi}_{\sigma_2})|\Psi^{(+)'}_{\mathrm{dte}}\rangle|^2$. Hence, with (8) and (9), we get

$$\begin{aligned}
&\mathrm{P}^{(+)}_{\mathrm{dte}}(\sigma_1,\sigma_2|\ell_1,\ell_2)\\
&\quad= \frac{1}{4}\Big[1+\sigma_1\sigma_2\mathrm{Re}\Big\{\mathrm{e}^{-\mathrm{i}\phi_\tau}\Big\langle\Psi_0^{(+)}\Big|\mathrm{e}^{\mathrm{i}\hat{p}_1\ell_1/\hbar}\mathrm{e}^{-\mathrm{i}\hat{p}_1^2\tau/2m\hbar}\\
&\qquad\otimes\mathrm{e}^{\mathrm{i}\hat{p}_2\ell_2/\hbar}\mathrm{e}^{-\mathrm{i}\hat{p}_2^2\tau/2m\hbar}\Big|\Psi_0^{(+)}\Big\rangle\Big\}\Big],
\end{aligned}$$

where we have for simplicity taken the beam splitters to be symmetric ($\theta_i=\pi/4$) and the particles to be of equal mass m. Evaluating the matrix element in momentum representation, with the abbreviations $\vec{p}=(p_1,p_2)^{\mathrm{T}}$ and $\vec{\ell}=(\ell_1,\ell_2)^{\mathrm{T}}$, yields

$$\begin{aligned}
&\mathrm{P}^{(+)}_{\mathrm{dte}}(\sigma_1,\sigma_2|\ell_1,\ell_2)\\
&\quad= \frac{1}{4}\Big[1+\sigma_1\sigma_2\mathrm{Re}\Big\{\mathrm{e}^{-\mathrm{i}\phi_\tau}\int_{-\infty}^{\infty}\mathrm{d}p_1\int_{-\infty}^{\infty}\mathrm{d}p_2\,\mathrm{e}^{\mathrm{i}\vec{p}\cdot\vec{\ell}/\hbar}\\
&\qquad\times\mathrm{e}^{-\mathrm{i}\vec{p}^2\tau/2m\hbar}\Big|\Big\langle p_1,p_2|\Psi_0^{(+)}\Big\rangle\Big|^2\Big\}\Big].
\end{aligned} \tag{10}$$

The intermediate result (10) already reveals some important features of the setup: Firstly, the overall free time evolution $\hat{\mathrm{U}}^{(0)}_t$ in (8) drops out for the detection probability, as it was the case for the TBE state. Hence, only the dispersion-induced distortion between the early and late wave packets, which is due to the period τ between the two dissociation processes, causes potential harm to the fringe pattern of the detection probability as a function of the arm length variations. Next, only the momentum distribution $|\langle p_1,p_2|\Psi_0^{(+)}\rangle|^2$ of the single dissociation pulse component $|\Psi_0^{(+)}\rangle$ enters the detection probability $\mathrm{P}^{(+)}_{\mathrm{dte}}(\sigma_1,\sigma_2|\ell_1,\ell_2)$. As a consequence, $\mathrm{P}^{(+)}_{\mathrm{dte}}(\sigma_1,\sigma_2|\ell_1,\ell_2)$ is invariant under momentum phase transformations $\langle p_1,p_2|\Psi_0\rangle \to \exp[\mathrm{i}\xi(p_1,p_2)]\langle p_1,p_2|\Psi_0\rangle$, which includes spatial translations. This means that the signal is unaffected by shot-to-shot shifts of the source position with respect to the interferometers (as long as the interferometric procedure is still feasible). The mere dependence on the momentum distribution also shows that it is straightforward to generalize the detection probability to nonpure and nonseparable states, $|\Psi_0^{(+)}\rangle\langle\Psi_0^{(+)}| \to \rho_0^{(+)}$, and correspondingly $|\langle p_1,p_2|\Psi_0^{(+)}\rangle|^2 \to \mathrm{pr}(p_1,p_2) := \langle p_1,p_2|\rho_0^{(+)}|p_1,p_2\rangle$.

In the end, we are interested in the functional dependence of the detection probability on the variations ℓ_i of the interferometer arm lengths. In order to get a qualitative and quantitative understanding of the resulting fringe pattern, we evaluate (10) in closed form for the case that the early and the late wave packet components are each described by a generic (mixed) Gaussian state. This is reasonable, since even for non-Gaussian wave packet components with a more complicated momentum distribution, an appropriate Gaussian fit should allow us to derive at least a lower bound to the quality of the fringe pattern. For a Gaussian momentum distribution,

$$\begin{aligned}
\mathrm{pr}(p_1,p_2) = &\frac{1}{2\pi\sigma_{p,\mathrm{cm}}\sigma_{p,\mathrm{rel}}}\\
&\times\exp\!\left(-\frac{(p_1+p_2)^2}{2\sigma^2_{p,\mathrm{cm}}}-\frac{(p_1-p_2-m\upsilon_{\mathrm{rel}})^2}{8\sigma^2_{p,\mathrm{rel}}}\right),
\end{aligned}$$

we arrive at

$$\begin{aligned}
&\mathrm{P}^{(+)}_{\mathrm{dte}}(\sigma_1,\sigma_2|\ell_1,\ell_2)\\
&\quad= \frac{1}{4}\Bigg\{1+\sigma_1\sigma_2\left(1+\frac{\tau^2}{T^2_{\mathrm{cm}}}\right)^{-1/4}\left(1+\frac{\tau^2}{T^2_{\mathrm{rel}}}\right)^{-1/4}\\
&\qquad\times\exp\Bigg[-\frac{T_{\mathrm{rel}}}{T^2_{\mathrm{rel}}+\tau^2}\frac{(\ell_1-\ell_2-\tau\upsilon_{\mathrm{rel}})^2}{2\upsilon_{\mathrm{rel}}\lambda\!\!\!^{-}_{\mathrm{rel}}}\\
&\qquad-\frac{T_{\mathrm{cm}}}{T^2_{\mathrm{cm}}+\tau^2}\frac{(\ell_1+\ell_2)^2}{2\upsilon_{\mathrm{rel}}\lambda\!\!\!^{-}_{\mathrm{rel}}}\Bigg]\\
&\qquad\times\cos\Bigg[\frac{\ell_1-\ell_2}{\lambda\!\!\!^{-}_{\mathrm{rel}}}+\frac{\tau}{T^2_{\mathrm{rel}}+\tau^2}\frac{(\ell_1-\ell_2-\tau\upsilon_{\mathrm{rel}})^2}{2\upsilon_{\mathrm{rel}}\lambda\!\!\!^{-}_{\mathrm{rel}}}\\
&\qquad+\frac{\tau}{T^2_{\mathrm{cm}}+\tau^2}\frac{(\ell_1+\ell_2)^2}{2\upsilon_{\mathrm{rel}}\lambda\!\!\!^{-}_{\mathrm{rel}}}-\frac{\varphi_0}{2}\Bigg]\Bigg\}
\end{aligned} \tag{11}$$

with $\varphi_0 = \tau\upsilon_{\mathrm{rel}}/\lambda\!\!\!^{-}_{\mathrm{rel}} + \arctan(\tau/T_{\mathrm{cm}}) + \arctan(\tau/T_{\mathrm{rel}}) + 2\phi_\tau$. The variances of the relative and the center-of-mass momentum, denoted by $\sigma_{p,\mathrm{rel}}$ and $\sigma_{p,\mathrm{cm}}$, respectively, determine characteristic dispersion times, $T_{\mathrm{cm}} = 2m\hbar/\sigma^2_{p,\mathrm{cm}}$ and $T_{\mathrm{rel}} = m\hbar/2\sigma^2_{p,\mathrm{rel}}$. The latter indicate the time scale of transition to a dispersion-dominated spatial extension of the wave packets. The expectation value of the relative momentum $p_{0,\mathrm{rel}} = m\upsilon_{\mathrm{rel}}/2$ defines the reduced wave length

$\lambda\!\!\!^{-}_{\mathrm{rel}} = \hbar/p_{0,\mathrm{rel}}$, which sets the scale for the nonlocal interference fringes.

The DTE detection probability (11) has the potential to violate a Bell inequality, as is seen from its structural similarity to the TBE detection probability (6). The dispersion-induced distortion between the early and the late wave packet components is reflected in those terms in (11) which depend on the characteristic dispersion times T_{cm} and T_{rel}. In particular, it is responsible for the overall suppression of the fringe pattern as described by the Lorentzian reduction factors. Further, it causes a quadratic compression of the fringe pattern. The additional Gaussian suppression is due to the unavoidable envelope mismatch that follows from the variation of the arm lengths.

In order to get an unambigous demonstration of nonlocal correlations, the fringe visibility has to exceed the threshold value $1/\sqrt{2}$ over at least a few fringes when varying either arm length by ℓ_i. An analysis of the joint detection probability (11) shows that this is achieved given the following two conditions are met:

$$\lambda\!\!\!^{-}_{\mathrm{rel}}/(\tau v_{\mathrm{rel}}) \ll 1, \tag{12}$$

$$\left(1+\tau^2/T_{\mathrm{cm}}^2\right)\left(1+\tau^2/T_{\mathrm{rel}}^2\right) < 4. \tag{13}$$

So far, we have restricted our investigation to the DTE state $|\Psi_{\mathrm{dte}}^{(+)}\rangle$ with each particle propagating into a given direction. It is clear that we could have followed the same reasoning for the DTE state $|\Psi_{\mathrm{dte}}^{(-)}\rangle$, only with the labels for the particles exchanged, so that the corresponding joint detection probability $\mathrm{P}_{\mathrm{dte}}^{(-)}(\sigma_1,\sigma_2|\ell_1,\ell_2)$ equals $\mathrm{P}_{\mathrm{dte}}^{(+)}(\sigma_1,\sigma_2|\ell_1,\ell_2)$. Finally, since no interference between $|\Psi_{\mathrm{dte}}^{(+)}\rangle$ and $|\Psi_{\mathrm{dte}}^{(-)}\rangle$ occurs in our setup, the detection probability for the symmetric DTE state $|\Psi_{\mathrm{dte}}\rangle = \frac{1}{\sqrt{2}}(|\Psi_{\mathrm{dte}}^{(+)}\rangle + |\Psi_{\mathrm{dte}}^{(-)}\rangle)$ follows from

$$\begin{aligned}\mathrm{P}_{\mathrm{dte}}(\sigma_1,\sigma_2|\ell_1,\ell_2) &= \frac{1}{2}\Big(\mathrm{P}_{\mathrm{dte}}^{(+)}(\sigma_1,\sigma_2|\ell_1,\ell_2)\\ &\quad + \mathrm{P}_{\mathrm{dte}}^{(-)}(\sigma_1,\sigma_2|\ell_1,\ell_2)\Big)\\ &= \mathrm{P}_{\mathrm{dte}}^{(+)}(\sigma_1,\sigma_2|\ell_1,\ell_2).\end{aligned}$$

Hence, the results obtained for the directed DTE state $|\Psi_{\mathrm{dte}}^{(+)}\rangle$ apply just as well to the experimentally realized DTE state $|\Psi_{\mathrm{dte}}\rangle$.

We thus find that an unambigous verification of nonlocal correlations by violating a Bell inequality can be achieved in the setup considered above, given the conditions (12) and (13) are satisfied. A recent proposal is based on the Feshbach-induced dissociation of a molecular Bose–Einstein condensate [5]. As is argued there, an experiment based on fermionic Lithium atoms would indeed meet the above conditions (12) and (13), and hence raises hope for demonstrating nonclassicality in the motion of material particles. This setup would involve time separations between the two dissociation pulses on the order of seconds. This would result in a spatial separation between the early and late wave packets on the order of centimeters, rendering the DTE state truly macroscopic.

4 Conclusions

We presented a scheme to generate and verify nonlocal correlations between two material particles involving macroscopic superpositions of the spatial wave function. This is achieved by violating a Bell inequality using single-particle matter wave optics and simple position measurements. We conclude by summarizing the advantages of the presented scheme. First of all, it does not require interferometric stability between the two interferometers, which allows one to reach truly macroscopic separations. Moreover, the restriction to the coherence properties between the early and late wave packets as a whole means that only port-selective measurements are needed, requiring neither prominent spatial nor temporal resolution. This renders the nonclassical correlations largely independent of the shape of the wave packets and of the particular implementation of the position measurement. Finally, the low velocity of the propagating atoms in principle allows one to check the particle positions by laser illumination whenever one wishes. One might thus think of a demonstration experiment, where only after the dissociation of the particles the experimenter makes the conscious decision whether she wants to check the correlation of the emission times (by "looking" at the particles in front of the interferometers) or whether she wants to check the nonlocal correlations (by "looking" at the particles behind of the interferometers). This way, by performing such an experiment with proper, material particles and on truly macroscopic scales on the order of centimeters, nonclassical quantum correlations would be made amenable to anyone who understands the basic concept of the position of a particle, even to a layman who is ignorant of physics. All this renders the proposed setup a rather robust and striking test of nonclassicality in the motion of material particles with the potential to push the corresponding quantum regime into the macroscopic.

As an outlook, it would be illuminating to investigate the influence of various sources of decoherence. For the experimental proposal in [5], the effect of scattering of off-resonant photons and the scattering of background particles was already found to be controllable. In particular, it would be interesting to check to what degree the present setup can be used to test possible unconventional collapse theories, which predict a loss of coherence in the motion of material particles due to purported quantum gravity effects, on the centimeter scale accessible for the first time with the present measurement scheme.

References

1. A. Einstein, B. Podolsky, N. Rosen, Phys. Rev. **47**, 777 (1935)
2. E. Schrödinger, Proc. Camb. Philos. Soc. **31**, 555 (1935)
3. J.S. Bell, Physics **1**, 195 (1964)
4. A. Aspect, J. Dalibard, G. Roger, Phys. Rev. Lett. **49**, 1804 (1982)
5. C. Gneiting, K. Hornberger, Phys. Rev. Lett. **101**, 260503 (2008)
6. K.V. Kheruntsyan, M.K. Olsen, P.D. Drummond, Phys. Rev. Lett. **95**, 150405 (2005)
7. T. Opatrný, G. Kurizki, Phys. Rev. Lett. **86**, 3180 (2001)
8. K. Banaszek, K. Wodkiewicz, Phys. Rev. A **58**, 4345 (1998)
9. Z.-B. Chen, J.-W. Pan, G. Hou, Y.-D. Zhang, Phys. Rev. Lett. **88**, 040406 (2002)
10. J. Brendel, N. Gisin, W. Tittel, H. Zbinden, Phys. Rev. Lett. **82**, 2594 (1999)
11. W. Tittel, J. Brendel, H. Zbinden, N. Gisin, Phys. Rev. Lett. **84**, 4737 (2000)
12. C. Simon, J.P. Poizat, Phys. Rev. Lett. **94**, 030502 (2005)
13. J.D. Franson, Phys. Rev. Lett. **62**, 2205 (1989)
14. T. Mukaiyama, J. Abo-Shaeer, K. Xu, J. Chin, W. Ketterle, Phys. Rev. Lett. **92**, 180402 (2004)
15. S. Dürr, T. Volz, G. Rempe, Phys. Rev. A **70**, 031601 (2004)
16. G.R. Allcock, Ann. Phys. **53**, 253 (1969)
17. R. Werner, J. Math. Phys. **27**, 793 (1986)
18. Y. Aharonov, J. Oppenheim, S. Popescu, B. Reznik, W.G. Unruh, Phys. Rev. A **57**, 4130 (1998)
19. J.G. Muga, C.R. Leavens, Phys. Rep. **338**, 353 (2000)
20. J.F. Clauser, M.A. Horne, A. Shimony, R.A. Holt, Phys. Rev. Lett. **23**, 880 (1969)
21. S. Aerts, P. Kwiat, J.-A. Larsson, M. Żukowski, Phys. Rev. Lett. **83**, 2872 (1999)
22. A. Cabello, A. Rossi, G. Vallone, F. De Martini, P. Mataloni, Phys. Rev. Lett. **102**, 040401 (2009)
23. J.R. Taylor, *Scattering Theory: The Quantum Theory on Nonrelativistic Collisions* (Wiley, New York, 1972)